

## Chemoinformatic-aided Antidiabetic Analysis of the Therapeutic Potential of Phytoconstituents in *Eremomastax speciosa* Extracts

Sulyman Olalekan Ibrahim <sup>1\*</sup>  

Halimat Yusuf Lukman <sup>2</sup>  

Israel Ehizuelen Ebhohimen <sup>3</sup>  

Halimah Funmilayo Babamale <sup>1</sup>  

Fatimah Ronke Abdulkadir <sup>4</sup> 

Abdulmumeen Amao Hamid <sup>4</sup>  

Marili Funmilayo Zubair <sup>1</sup>  

Olubunmi Atolani <sup>4</sup>  

<sup>1</sup> Department of Industrial Chemistry, University of Ilorin, Ilorin, Kwara State, Nigeria

<sup>2</sup> Department of Chemical Sciences, Summit University, Offa, Kwara State, Nigeria

<sup>3</sup> Department of Biochemistry, Ambrose Alli University, Ekpoma, Edo State, Nigeria

<sup>4</sup> Department of Chemistry, University of Ilorin, Ilorin, Kwara State, Nigeria

\*email: [ibrahim.sio@unilorin.edu.ng](mailto:ibrahim.sio@unilorin.edu.ng); phone: +2348030661412

### Keywords:

$\alpha$ -amylase  
Antihyperglycemic  
Metformin  
Molecular docking  
Phytochemicals

### Abstract

This research attempts to establish the antihyperglycemic potential of *Eremomastax speciosa*, a medicinal plant utilized in traditional West African diabetes therapy, through virtual simulation. While numerous reports have validated its biological potency, studies on the drug-likeness and antidiabetic properties of its compounds are limited. The *in silico* pharmacological, and toxicological profile of aqueous, methanolic/methylene phytochemicals from previously reported work was analyzed using Swiss ADME and Protox II online server. The docking process was performed using PyRx-0.8, coupled with AutoDock Vina. Phytochemicals that aligned with Lipinski's rules for drugs were then subjected to a virtual docking simulation. This simulation replicated the inhibitory effects of *E. speciosa* phytochemicals on sodium-glucose co-transporters (SGLT2) and  $\alpha$ -amylase, similar to metformin, an FDA-approved antidiabetic medicine utilized as a control. Phytochemicals such as 8, 9,10-dimethyltricyclo[4.2.1.1(2,5)]decane-9,10-diol (-6.6 kcal/mol), 11-isopropylidenetricyclo[4.3.1.1(2,5)]undec-3-en-10-one (-7.9 kcal/mol), 4-(1,5-dihydroxy-2,6,6-trimethylcyclohex-2-enyl)but-3-en-2-one (-7.3 kcal/mol), and N-methyl-N-4-[2-acetoxymethyl-1-pyrrolidyl]-2-butynyl]-acetamide (-7.5 kcal/mol) exhibits superior binding affinities to the specific proteins targeted, compared to metformin, implying that *E. speciosa* is a source of druggable antidiabetic molecules that can be enhanced to achieve better efficacy.

Received: March 10<sup>th</sup>, 2024

1<sup>st</sup> Revised: May 13<sup>th</sup>, 2024

Accepted: May 20<sup>th</sup>, 2024

Published: May 30<sup>th</sup>, 2024



© 2024 Sulyman Olalekan Ibrahim, Halimat Yusuf Lukman, Israel Ehizuelen Ebhohimen, Halimah Funmilayo Babamale, Fatimah Ronke Abdulkadir, Abdulmumeen Amao Hamid, Marili Funmilayo Zubair, Olubunmi Atolani. Published by Institute for Research and Community Services Universitas Muhammadiyah Palangkaraya. This is an Open Access article under the CC-BY-SA License (<http://creativecommons.org/licenses/by-sa/4.0/>). DOI: <https://doi.org/10.33084/bjop.v7i2.6820>

## INTRODUCTION

Diabetes mellitus, a chronic metabolic disorder characterized by hyperglycemia, remains a global health crisis<sup>1,2</sup>. The vast majority (>95%) of diabetes cases are diagnosed as type 2 diabetes mellitus (T2DM), resulting from insulin resistance and impaired pancreatic  $\beta$ -cell function<sup>3,4</sup>. This condition significantly contributes to morbidity and mortality worldwide<sup>5</sup>. While various treatment options exist, including insulin preparations and synthetic oral hypoglycemics, the discovery and development of novel antidiabetic medications remains a research priority<sup>6</sup>.

Plants have long been recognized for their potential to treat and manage various ailments<sup>7</sup>. Notably, medicinal plants have been documented to possess insulin-mimicking properties, regulate insulin secretion, and inhibit carbohydrate-digesting enzymes, making them promising candidates for exploring and developing new diabetes therapies<sup>8</sup>. *Eremomastax speciosa*, also known as "Edem Iduodut" or "Ndadad Edem" among the Ibibio people of Nigeria and as "African blood tonic" in

Cameroon, is an indigenous plant native to tropical regions, particularly Africa<sup>9</sup>. Traditionally, its leaves and roots are used in decoctions, infusions, or poultices to treat various illnesses, including diabetes, anemia, constipation, diarrhea, and malaria<sup>10,11</sup>. The lack of scientific data regarding the antidiabetic potential and the absorption, distribution, metabolism, excretion, and toxicity (ADMET) properties of its bioactive compounds necessitates further investigation.

Advancements in computer technology have facilitated the use of *in silico* methods, such as virtual screening and network analysis, to investigate the pharmacological and therapeutic potential of phytochemicals found in medicinal plants<sup>12,13</sup>. These computational tools enable the rapid prediction of phytochemicals with promising pharmacological profiles, potentially accelerating the discovery of novel and more effective plant-derived antidiabetic drugs<sup>14</sup>. Establishing a streamlined approach for the initial *in silico* prediction of bioactive compounds, followed by subsequent *in vitro* and *in vivo* validation, has the potential to significantly improve the efficiency of evaluating the medicinal properties of plants<sup>15</sup>. This study aims to utilize online servers and molecular docking simulations to evaluate the ADMET, pharmacokinetics, and drug-likeness properties of bioactive compounds identified in *E. speciosa*. Additionally, we investigate the plant's potential antidiabetic activity using *in silico* methods.

## MATERIALS AND METHODS

### Materials

The computational analyses were performed on a Lenovo T460 personal computer equipped with an Intel® Core™ i5-6300U CPU (2.4-2.5 GHz, 6<sup>th</sup> generation), 16 GB RAM, and a 64-bit operating system with an x64-based processor running Microsoft Windows 10. The following software programs were utilized, including ChemDraw Ultra v.12.0, PyRx-0.8 software coupled with AutoDock Vina 1.1.2, and BIOVIA Discovery Studio Visualizer v.16.1.0.1535. Online web servers were employed for property prediction and toxicity analysis, including SwissADME (<http://www.swissadme.ch/index.php>), ProTox II ([https://tox-new.charite.de/protox\\_II/index.php?site=compound\\_input](https://tox-new.charite.de/protox_II/index.php?site=compound_input)), ChEMBL (<https://www.ebi.ac.uk/chembl/>), and PubChem (<https://pubchem.ncbi.nlm.nih.gov/>).

### Methods

#### Data mining of *E. speciosa* phytochemicals

Information regarding the bioactive phytochemicals present in *E. speciosa* was obtained from a literature review conducted by Siwe *et al.*<sup>16</sup>. This review identified ten phytochemicals reported in the aqueous extract and 14 phytochemicals reported in the methanolic/methylene extract. This dataset of twenty-four putatively bioactive compounds formed the basis for the current study.

#### Prediction of ADME and toxicity

The SwissADME was employed to predict the physicochemical properties, ADME parameters, and drug-likeness of the identified small phytochemicals<sup>17</sup>. This online platform facilitates the exploration of these properties, aiding in the drug discovery process. Canonical SMILES strings generated using ChemDraw were uploaded into SwissADME to obtain predictions for physicochemical properties (e.g., lipophilicity, water solubility), pharmacokinetics, drug-likeness, and medicinal chemistry friendliness. To assess the potential *in silico* toxicity profile of the identified compounds, the canonical SMILES formula obtained from ChemDraw was used for analysis with Protox II<sup>18</sup>.

#### Retrieval, preparation, and identification of protein active sites

To predict the potential antidiabetic properties of the identified druggable phytochemicals from *E. speciosa*, we employed *in silico* molecular docking simulations. Metformin and acarbose, established antidiabetic drugs, were used as references to understand their mechanisms of action. Information regarding their mechanisms was retrieved from the ChEMBL database. Metformin is known to inhibit sodium-glucose co-transporter 2 (SGLT2)<sup>19</sup>, while acarbose acts as an  $\alpha$ -amylase inhibitor<sup>20</sup>. The crystal structures of human SGLT2 (PDB ID 8HDF1) and  $\alpha$ -amylase (PDB ID 4GQR) were obtained from the Protein Data Bank (<https://www.rcsb.org/>). These protein structures were then optimized for docking simulations. The binding site coordinates for each enzyme were identified by analyzing the co-crystallized inhibitors within the respective

protein structures, utilizing the Discovery Studio Visualizer. Docking simulations were performed for each phytochemical against SGLT2 and  $\alpha$ -amylase. The docking scores and the most favorable binding poses for each complex were documented<sup>21</sup>.

#### Ligand preparation and molecular docking

To gain insights into the potential mechanisms of action of the identified phytochemicals, *in silico* docking simulations were performed. The known mechanisms of standard drugs metformin (SGLT2 inhibitor) and acarbose ( $\alpha$ -amylase inhibitor) were retrieved from the ChEMBL database. Crystal structures of these standard drugs, along with all phytochemicals identified through GC-MS analysis, were downloaded in SDF format from PubChem. Open Babel was employed to prepare and optimize the downloaded structures for docking simulations. The PyRx platform coupled with AutoDock Vina was then utilized for docking simulations. Briefly, the phytoconstituents isolated from the methanolic and aqueous extracts of *E. speciosa* were docked into the active sites of human  $\alpha$ -amylase and SGLT2. The protein structures used for docking were retrieved from the Protein Data Bank, focusing on co-crystallized forms to incorporate the bound ligand information. The specific amino acid residues constituting the active sites were selected based on the downloaded PDB structures<sup>22</sup>.

#### Data analysis

Following the docking simulations, the ligand-protein complex with the most favorable binding affinity ( $\Delta G$ ; kcal/mol) and pose was selected. This complex was then saved in the PDB file format for further analysis. The Discovery Studio Visualizer was employed to visualize and analyze the intermolecular interactions formed between the ligands and the target protein<sup>23</sup>.

## RESULTS AND DISCUSSION

**Tables I to VI** detail the physicochemical properties of the aqueous extract (AES) and methanolic extract (MES) of *E. speciosa*. While some compounds were identified in both extracts, independent analysis was conducted to establish a reference library of compounds present in each. Molecular weight (MW) is a crucial physicochemical property affecting processes like absorption and interaction with targets<sup>24,25</sup>. Lipinski's rule of five suggests favorable drug-like properties for compounds with MW below 500 Da, logP less than 5, and a limited number of hydrogen bond donors and acceptors<sup>13,26,27</sup>. All identified *E. speciosa* phytochemicals complied with these rules, indicating good oral bioavailability potential. The majority of identified compounds in the AES, with the exception of trilinolein (MW 879.83 g/mol, rotatable bonds 50, relative formula mass (MR) >250, and heavy atom 63), exhibited a molecular weight below 500 g/mol and an atomic weight <40. Additionally, all AES compounds possessed a topological polar surface area (TPSA) below 100 and contained a limited number of hydrogen bond acceptors and donors (less than 10 and 5, respectively). Notably, the physicochemical properties of the MES compounds followed a similar trend, with the exception of 4,22-cholestadien-3-one, which displayed a molecular weight exceeding 500 g/mol (**Tables I and II**).

**Table I.** Physicochemical properties of phytochemicals from AES.

Phytochemicals	MW	#Heavy atoms	#Aromatic heavy atoms	Fraction Csp3	#Rotatable bonds	#H-bond acceptors	#H-bond donors	MR	TPSA
9-oxabicyclo[3.3.1]nonane-2,6-diol	158.19	11	0	1	0	3	2	39.75	49.69
2,7-dioxaisotwistane	140.18	10	0	1	0	2	0	36.4	18.46
5-hydroxy-9-oxabicyclo[3.3.1]nonan-2-one	156.18	11	0	0.88	0	3	1	38.83	46.53
11-isopropylidenetricyclo[4.3.1.1(2,5)]undec-3-en-10-one	202.29	15	0	0.64	0	1	0	62.32	17.07
4-(1,5-dihydroxy-2,6,6-trimethylcyclohex-2-enyl)but-3-en-2-one	224.3	16	0	0.62	2	3	2	63.84	57.53
7-methyl-Z-tetradecen-1-ol acetate	268.43	19	0	0.82	13	2	0	84.64	26.3
ethyl iso-allocholate	436.62	31	0	0.96	6	5	3	122.89	86.99
Trilinolein	879.38	63	0	0.74	50	6	0	277.12	78.9
Olean-12-en-3-one	424.7	31	0	0.9	0	1	0	133.92	17.07
$\alpha$ -amyrin	426.72	31	0	0.93	0	1	1	135.14	20.23

**Table II.** Physicochemical properties of phytochemicals from MES.

Phytochemicals	MW	#Heavy atoms	#Aromatic heavy atoms	Fraction Csp3	#Rotatable bonds	#H-bond acceptors	#H-bond donors	M R	TPSA
9-oxabicyclo[3.3.1]nonane-2,6-diol	158.19	11	0	1	0	3	2	39.75	49.69
2,5-methano-2H-furo[3,2-b]pyran, hexahydro (2,7-dioxaisotwistane)	140.18	10	0	1	0	2	0	36.4	18.46
6,6-dimethyl-10-methylene-1-oxa-spiro[4.5]decane	180.29	13	0	0.83	0	1	0	55.96	9.23
N-methyl-N-[4-[2-acetoxymethyl-1-pyrrolidyl]-2-butynyl]-acetamide	266.34	19	0	0.71	6	4	0	76.65	49.85
9,10-dimethyltricyclo[4.2.1.1(2,5)]decane-9,10-diol	196.29	14	0	1	0	2	2	55.86	40.46
2-pentadecanone, 6,10,14-trimethyl	268.48	19	0	0.94	12	1	0	88.84	17.07
Phytol	296.53	21	0	0.9	13	1	1	98.94	20.23
Isophytol	296.53	21	0	0.9	13	1	1	98.98	20.23
Z-(13,14-epoxy)tetradec-11-en-1-ol acetate	268.39	19	0	0.81	13	3	0	78.81	38.83
E,Z-1,3,12-nonadecatriene	294.47	21	0	0.68	14	2	2	94.35	40.46
7-methyl-Z-tetradecen-1-ol acetate	268.43	19	0	0.82	13	2	0	84.64	26.3
Ethyl iso-allocholate	424.7	31	0	0.9	1	1	0	134.18	17.07
Lupenone	382.62	28	0	0.81	4	1	0	122.18	17.07
4,22-cholestadien-3-one	502.77	36	0	0.97	7	4	1	147.9	59.06

**Tables III and IV** present the MLOGP values for the identified phytochemicals in AES and MES. These values indicate the relative preference of a compound for partitioning between lipophilic (fatty) and hydrophilic (watery) environments. Generally, the phytochemicals in AES exhibited significant lipophilicity, with most MLOGP values falling below 4.5 (**Table III**). This suggests that these compounds preferentially partition into the lipophilic phase, potentially favoring absorption across cell membranes. Exceptions include trilinolein, olean-12-en-3-one, and  $\alpha$ -amyirin. Conversely, MES displayed a trend towards higher lipophilicity, with a few compounds, such as ethyl iso-allocholate and lupenone, having MLOGP values exceeding 4.5 (**Table IV**).

**Table III.** Lipophilicity properties of phytochemicals from AES.

Phytochemicals	iLOG P	XLOGP 3	WLOG P	MLOG P	Silicos-IT LogP	Consensus LogP
9-oxabicyclo[3.3.1]nonane-2,6-diol	1.53	-0.05	0.05	0.02	0.38	0.38
2,7-dioxaisotwistane	2.01	0.95	1.1	0.9	1.53	1.3
5-hydroxy-9-oxabicyclo[3.3.1] nonan-2-one	0.9	0.16	0.61	0.28	1.36	0.66
11-isopropylidene-tricyclo [4.3.1.1(2,5)]undec-3-en-10-one	2.48	2.77	3.12	3.21	2.83	2.88
4-(1,5-dihydroxy-2,6,6-trimethylcyclohex-2-enyl)but-3-en-2-one	2.29	0.72	1.6	1.14	2.04	1.56
7-methyl-Z-tetradecen-1-ol acetate	3.74	6.18	5.27	4.33	5.49	5
ethyl iso-allocholate	3.99	2.71	3.93	3.46	3.49	3.52
Trilinolein	12.82	20.34	17.43	9.25	20.55	16.08
Olean-12-en-3-one	4.53	8.84	8.38	6.82	7.51	7.21
$\alpha$ -amyirin	4.77	9.01	8.02	6.92	6.52	7.05

**Table IV.** Lipophilicity properties of phytochemicals from MES.

Phytochemicals	iLOG P	XLOGP 3	WLOG P	MLOG P	Silicos-IT LogP	Consensus LogP
9-oxabicyclo[3.3.1]nonane-2,6-diol	1.53	-0.05	0.05	0.02	0.38	0.38
2,5-methano-2H-furo[3,2-b]pyran, hexahydro (2,7-dioxaisotwistane)	2.01	0.95	1.1	0.9	1.53	1.3
6,6-dimethyl-10-methylene-1-oxa-spiro[4.5]decane	2.75	2.81	3.3	2.88	3.65	3.08
N-methyl-N-[4-[2-acetoxymethyl-1-pyrrolidyl]-2-butynyl]-acetamide	3.01	0.27	0.19	0.94	1.18	1.12
9,10-dimethyltricyclo[4.2.1.1(2,5)]decane-9,10-diol	2.33	1.14	1.55	2.09	1.68	1.76
2-pentadecanone, 6,10,14-trimethyl	4.39	6.95	6.01	4.79	6.18	5.66
Phytol	4.71	8.19	6.36	5.25	6.57	6.22
Isophytol	4.88	7.83	6.36	5.25	6.57	6.18
Z-(13,14-epoxy)tetradec-11-en-1-ol acetate	268.39	19	0	0.81	13	3
E,Z-1,3,12-nonadecatriene	294.47	21	0	0.68	14	2
7-methyl-Z-tetradecen-1-ol acetate	268.43	19	0	0.82	13	2
Ethyl iso-allocholate	424.7	31	0	0.9	1	1
Lupenone	382.62	28	0	0.81	4	1
4,22-cholestadien-3-one	502.77	36	0	0.97	7	4

Water solubility is another critical factor for absorption and drug formulation<sup>28</sup>. While specific solubility values were not determined, the presence of these compounds in hydrophilic extracts suggests favorable interaction with the aqueous environment, potentially enhancing biological activity. SwissADME predictions indicated solubility ranging from low to moderate for various compounds, suggesting potential for bioabsorption and diverse therapeutic applications depending on solubility characteristics. **Tables V** and **VI** present the hydrophilicity properties of AES and MES, respectively. As expected, all extracts exhibited good solubility in water due to their hydrophilic nature. Investigating the potential for drug interactions, we evaluated the inhibitory effects of these extracts on cytochrome P450 (CYP) isoenzymes. Interestingly, none of the compounds identified in AES showed any inhibitory activity against CYP isoenzymes (**Table VII**).

Gastrointestinal absorption (GIA), blood-brain barrier (BBB) permeability, and P-glycoprotein (P-gp) substrate potential were evaluated using *in silico* tools. Additionally, all AES components displayed favorable absorption characteristics, with high GIA and the ability to permeate BBB, except for trilinolein, olean-12-en-3-one, and  $\alpha$ -amyrin. In contrast, the analysis of MES components revealed that most exhibited significant inhibition of the CYP2C9 isoenzyme, potentially leading to drug interactions (**Table VIII**). Despite this concern, MES components generally demonstrated favorable ADME profiles, with high GIA and BBB permeability. Notably, ethyl iso-allocholate, lupenone, and 4,22-cholestadien-3-one deviated from this trend, displaying non-permeability to glycoprotein substrates. Generally, the compounds exhibited high predicted GIA, indicating good oral bioavailability<sup>29</sup>. Exceptions included trilinolein, olean-12-en-3-one,  $\alpha$ -amyrin, and several others, suggesting these compounds may require alternative administration routes or formulation strategies for optimal bioavailability. Most compounds were predicted to be non-BBB permeant, potentially limiting their utility for central nervous system (CNS)-related conditions<sup>30</sup>. However, some compounds with lower molecular weight and fewer hydrogen bonds might have the potential to cross the BBB for targeted brain therapies<sup>31</sup>. P-glycoprotein is an efflux pump that limits intestinal absorption of certain drugs. While some *E. speciosa* compounds were predicted P-gp substrates, further investigation is needed to determine the practical impact on their bioavailability.

**Table V.** Water solubility properties of phytochemicals from AES.

Phytochemicals	ESOL LogS	ESOL Solubility (mg/mL)	ESOL Solubility (mol/L)	ESOL Class	Ali LogS	Ali Solubility (mg/mL)	Ali Solubility (mol/L)	Ali Class	Silicos-IT LogSw	Silicos-IT Solubility	Silicos-IT Solubility (mol/L)	Silicos-IT class
9-oxabicyclo[3.3.1]nonane-2,6-diol	-0.79	2.57E+01	1.62E-01	Very soluble	-0.54	4.53E+01	2.87E-01	Very soluble	0.25	2.79E+02	1.76E+00	Soluble
2,7-dioxaisotwistane	-1.31	6.90E+00	4.92E-02	Very soluble	-0.92	1.67E+01	1.19E-01	Very soluble	-0.62	3.35E+01	2.39E-01	Soluble
5-hydroxy-9-oxabicyclo[3.3.1]nonan-2-one	-0.91	1.93E+01	1.23E-01	Very soluble	-0.69	3.16E+01	2.02E-01	Very soluble	-0.9	1.98E+01	1.27E-01	Soluble
11-isopropylidenedicyclo[4.3.1.1(2,5)]undec-3-en-10-one	-2.84	2.93E-01	1.45E-03	Soluble	-2.78	3.33E-01	1.64E-03	Soluble	-2.24	1.17E+00	5.81E-03	Soluble
4-(1,5-dihydroxy-2,6,6-trimethylcyclohex-2-enyl)but-3-en-2-one	-1.55	6.29E+00	2.80E-02	Very soluble	-1.51	6.99E+00	3.12E-02	Very soluble	-1.49	7.26E+00	3.24E-02	Soluble
7-methyl-Z-tetradecen-1-ol acetate	-4.54	7.75E-03	2.89E-05	Moderately soluble	-6.52	8.17E-05	3.04E-07	Poorly soluble	-4.92	3.24E-03	1.21E-05	Moderately soluble
ethyl iso-allocholate	-3.86	6.05E-02	1.39E-04	Soluble	-4.19	2.82E-02	6.45E-05	Moderately soluble	-3.39	1.77E-01	4.05E-04	Soluble
Trilinolein	-14.81	1.37E-12	1.56E-15	Insoluble	-22.31	4.26E-20	4.84E-23	Insoluble	-	3.96E-13	4.50E-16	Insoluble
Olean-12-en-3-one	-8.04	3.85E-06	9.07E-09	Poorly soluble	-9.08	3.51E-07	8.26E-10	Poorly soluble	-7.86	5.86E-06	1.38E-08	Poorly soluble
$\alpha$ -amyrin	-8.16	2.94E-06	6.89E-09	Poorly soluble	-9.33	2.02E-07	4.72E-10	Poorly soluble	-6.71	8.23E-05	1.93E-07	Poorly soluble

**Table VI.** Water solubility properties of phytochemicals from MES.

Phytochemicals	ESOL LogS	ESOL Solubility (mg/mL)	ESOL Solubility (mol/L)	ESOL Class	Ali LogS	Ali Solubility (mg/mL)	Ali Solubility (mol/L)	Ali Class	Silicos-IT LogSw	Silicos-IT Solubility	Silicos-IT Solubility (mol/L)	Silicos-IT class
9-oxabicyclo[3.3.1]nonane-2,6-diol	-0.79	2.57E+01	1.62E-01	Very soluble	-0.54	4.53E+01	2.87E-01	Very soluble	0.25	2.79E+02	1.76E+00	Soluble
2,5-methano-2H-furo[3,2-b]pyran, hexahydro (2,7-dioxaisotwistane)	-1.31	6.90E+00	4.92E-02	Very soluble	-0.92	1.67E+01	1.19E-01	Very soluble	-0.62	3.35E+01	2.39E-01	Soluble
6,6-dimethyl-10-methylene-1-oxa-spiro[4.5]decane	-2.73	3.37E-01	1.87E-03	Soluble	-2.66	3.94E-01	2.18E-03	Soluble	-3.25	1.00E-01	5.57E-04	Soluble
N-methyl-N-[4-[2-acetoxymethyl-1-pyrrolidyl]-2-butynyl]-acetamide	-1.27	1.45E+01	5.43E-02	Very soluble	-0.88	3.53E+01	1.32E-01	Very soluble	-1.53	7.86E+00	2.95E-02	Soluble
9,10-dimethyltricyclo[4.2.1.1(2,5)]decane-9,10-diol	-1.78	3.29E+00	1.68E-02	Very soluble	-1.58	5.12E+00	2.61E-02	Very soluble	-1.33	9.12E+00	4.65E-02	Soluble
2-pentadecanone, 6,10,14-trimethyl	-5.09	2.18E-03	8.11E-06	Moderately soluble	-7.12	2.03E-05	7.56E-08	Poorly soluble	-5.55	7.50E-04	2.79E-06	Moderately soluble
Phytol	-5.98	3.10E-04	1.05E-06	Moderately soluble	-8.47	9.94E-07	3.35E-09	Poorly soluble	-5.51	9.06E-04	3.05E-06	Moderately soluble
Isophytol	-5.75	5.23E-04	1.76E-06	Moderately soluble	-8.1	2.35E-06	7.92E-09	Poorly soluble	-5.51	9.06E-04	3.05E-06	Moderately soluble
Z-(13,14-epoxy)tetradec-11-en-1-ol acetate	-3.49	8.74E-02	3.26E-04	Soluble	-5.05	2.41E-03	8.98E-06	Moderately soluble	-4.16	1.87E-02	6.98E-05	Moderately soluble
E,Z-1,3,12-nonadecatriene	-4.31	1.45E-02	4.93E-05	Moderately soluble	-6.27	1.57E-04	5.32E-07	Poorly soluble	-3.88	3.88E-02	1.32E-04	Soluble
7-methyl-Z-tetradecen-1-ol acetate	-4.54	7.75E-03	2.89E-05	Moderately soluble	-6.52	8.17E-05	3.04E-07	Poorly soluble	-4.92	3.24E-03	1.21E-05	Moderately soluble
Ethyl iso-allocholate	-8.43	1.58E-06	3.72E-09	Poorly soluble	-9.83	6.28E-08	1.48E-10	Poorly soluble	-7.44	1.54E-05	3.63E-08	Poorly soluble
Lupenone	-6.69	7.89E-05	2.06E-07	Poorly soluble	-7.71	7.41E-06	1.94E-08	Poorly soluble	-5.75	6.74E-04	1.76E-06	Moderately soluble
4,22-cholestadien-3-one	-7.68	1.05E-05	2.09E-08	Poorly soluble	-9.33	2.34E-07	4.66E-10	Poorly soluble	-6.62	1.21E-04	2.41E-07	Poorly soluble

**Table VII.** Pharmacokinetics properties of phytochemicals from AES.

Phytochemicals	GI absorption	BBB permeant	Pgp substrate	CYP1A2 inhibitor	CYP2C19 inhibitor	CYP2C9 inhibitor	CYP2D6 inhibitor	CYP3A4 inhibitor	log Kp (cm/s)
9-oxabicyclo[3.3.1]nonane-2,6-diol	High	No	No	No	No	No	No	No	-7.3
2,7-dioxaisotwistane	High	Yes	No	No	No	No	No	No	-6.48
5-hydroxy-9-oxabicyclo[3.3.1]nonan-2-one	High	Yes	No	No	No	No	No	No	-7.14
11-isopropylideneditricyclo[4.3.1.1(2,5)]undec-3-en-10-one	High	Yes	No	No	Yes	No	No	No	-5.57
4-(1,5-dihydroxy-2,6,6-trimethylcyclohex-2-enyl)but-3-en-2-one	High	Yes	No	No	No	No	No	No	-7.16
7-methyl-Z-tetradecen-1-ol acetate	High	Yes	No	No	No	Yes	No	No	-3.55
ethyl iso-allocholate	High	No	Yes	No	No	No	No	No	-7.04
Trilinolein	Low	No	Yes	No	No	No	No	No	2.78
Olean-12-en-3-one	Low	No	No	No	No	No	No	No	-2.61
α-amyrin	Low	No	No	No	No	No	No	No	-2.51

**Table VIII.** Pharmacokinetics properties of phytochemicals from MES.

Phytochemicals	GI absorption	BBB permeant	Pgp substrate	CYP1A2 inhibitor	CYP2C19 inhibitor	CYP2C9 inhibitor	CYP2D6 inhibitor	CYP3A4 inhibitor	log Kp (cm/s)
9-oxabicyclo[3.3.1]nonane-2,6-diol	High	No	No	No	No	No	No	No	-7.3
2,5-methano-2H-furo[3,2-b]pyran, hexahydro (2,7-dioxaisotwistane)	High	Yes	No	No	No	No	No	No	-6.48
6,6-dimethyl-10-methylene-1-oxa-spiro[4.5]decane	High	Yes	No	No	No	Yes	No	No	-5.4
N-methyl-N-[4-[2-acetoxymethyl-1-pyrrolidyl]-2-butynyl]-acetamide	High	No	No	No	No	No	No	No	-7.73
9,10-dimethyltricyclo[4.2.1.1(2,5)]decane-9,10-diol	High	Yes	No	No	No	No	No	No	-6.69
2-pentadecanone, 6,10,14-trimethyl	High	No	Yes	No	No	Yes	No	No	-3
Phytol	Low	No	Yes	No	No	Yes	No	No	-2.29
Isophytol	Low	No	Yes	No	No	Yes	No	No	-2.55
Z-(13,14-epoxy)tetradec-11-en-1-ol acetate	High	Yes	No	Yes	No	Yes	Yes	No	-4.74
E,Z-1,3,12-nonadecatriene	High	Yes	Yes	Yes	No	Yes	Yes	Yes	-4.08

7-methyl-Z-tetradecen-1-ol acetate	High	Yes	No	No	No	Yes	No	No	-3.55
Ethyl iso-allocholate	Low	No	No	No	No	No	No	No	-2.1
Lupenone	Low	No	No	No	No	Yes	No	No	-3.29
4,22-cholestadien-3-one	Low	No	No	No	No	No	No	No	-3.52

Analysis based on Lipinski's Rule of Five indicated that all identified compounds within the extracts adhered to this rule, violating no more than two of its criteria (Tables IX and X). This suggests favorable drug-likeness properties, implying potential for oral bioavailability. Additionally, the extracts exhibited significant bioavailability scores, further supporting their potential for drug development. With the exception of trilinolein and 4,22-cholestadien-3-one, which displayed synthetic accessibility scores of 8.46 and 6.78, respectively, all other identified compounds possessed values <6.5. Lower synthetic accessibility scores generally indicate greater ease of synthesis. Furthermore, none of the identified compounds triggered a pain alert, suggesting a favorable safety profile (Tables XI and XII). This absence of pain alerts is a promising finding for the potential development of these compounds into safe and efficacious drugs. The combined analysis using Lipinski's rule, bioavailability scores, and ProTox-II predictions suggests that the identified *E. speciosa* phytochemicals possess promising drug-like properties and low predicted toxicity<sup>18</sup>. These findings indicate their potential as safe and viable candidates for further drug development.

**Table IX.** Drug-likeness and bioavailability score of phytochemicals from AES.

Phytochemicals	Lipinski #violations	Ghose #violations	Veber #violations	Egan #violations	Muegge #violations	Bioavailability Score
9-oxabicyclo[3.3.1]nonane-2,6-diol	0	2	0	0	1	0.55
2,7-dioxaisotwistane	0	2	0	0	1	0.55
5-hydroxy-9-oxabicyclo[3.3.1]nonan-2-one	0	2	0	0	1	0.55
11-isopropylidene-tricyclo[4.3.1.1(2,5)]undec-3-en-10-one	0	0	0	0	1	0.55
4-(1,5-dihydroxy-2,6,6-trimethylcyclohex-2-enyl)but-3-en-2-one	0	0	0	0	0	0.55
7-methyl-Z-tetradecen-1-ol acetate	1	0	1	0	1	0.55
ethyl iso-allocholate	0	1	0	0	0	0.55
Trilinolein	2	4	1	1	3	0.17
Olean-12-en-3-one	1	3	0	1	2	0.55
$\alpha$ -amyrin	1	3	0	1	2	0.55

**Table X.** Drug-likeness and bioavailability score of phytochemicals from MES.

Phytochemicals	Lipinski #violations	Ghose #violations	Veber #violations	Egan #violations	Muegge #violations	Bioavailability Score
9-oxabicyclo[3.3.1]nonane-2,6-diol	0	2	0	0	1	0.55
2,5-methano-2H-furo[3,2-b]pyran, hexahydro (2,7-dioxaisotwistane)	0	2	0	0	1	0.55
6,6-dimethyl-10-methylene-1-oxa-spiro[4.5]decane	0	0	0	0	2	0.55
N-methyl-N-[4-[2-acetoxymethyl-1-pyrrolidyl]-2-butynyl]-acetamide	0	0	0	0	0	0.55
9,10-dimethyltricyclo[4.2.1.1(2,5)]decane-9,10-diol	0	0	0	0	1	0.55
2-pentadecanone, 6,10,14-trimethyl	1	1	1	1	2	0.55
Phytol	1	1	1	1	2	0.55
Isophytol	1	1	1	1	2	0.55
Z-(13,14-epoxy)tetradec-11-en-1-ol acetate	0	0	1	0	0	0.55
E,Z-1,3,12-nonadecatriene	0	0	1	0	1	0.55
7-methyl-Z-tetradecen-1-ol acetate	1	0	1	0	1	0.55
Ethyl iso-allocholate	1	3	0	1	2	0.55
Lupenone	1	1	0	1	2	0.55
4,22-cholestadien-3-one	2	4	0	1	1	0.17

**Table XI.** Medicinal chemistry properties of phytochemicals from AES.

Phytochemicals	PAINS #alerts	Brenk #alerts	Leadlikeness #violations	Synthetic Accessibility
9-oxabicyclo[3.3.1]nonane-2,6-diol	0	2	0	0
2,7-dioxaisotwistane	0	2	0	0
5-hydroxy-9-oxabicyclo[3.3.1] nonan-2-one	0	2	0	0
11-isopropylidenetricyclo[4.3.1.1(2,5)]undec-3-en-10-one	0	0	0	0
4-(1,5-dihydroxy-2,6,6-trimethylcyclohex-2-enyl)but-3-en-2-one	0	0	0	0
7-methyl-Z-tetradecen-1-ol acetate	1	0	1	0
ethyl iso-allocholate	0	1	0	0
Trilinolein	2	4	1	1
Olean-12-en-3-one	1	3	0	1
$\alpha$ -amyrin	1	3	0	1

**Table XII.** Medicinal chemistry properties of phytochemicals from MES.

Phytochemicals	PAINS #alerts	Brenk #alerts	Leadlikeness #violations	Synthetic Accessibility
9-oxabicyclo[3.3.1]nonane-2,6-diol	0	2	0	0
2,5-methano-2H-furo[3,2-b]pyran, hexahydro (2,7-dioxaisotwistane)	0	2	0	0
6,6-dimethyl-10-methylene-1-oxa-spiro[4.5]decane	0	0	0	0
N-methyl-N-[4-[2-acetoxymethyl-1-pyrrolidyl]-2-butynyl]-acetamide	0	0	0	0
9,10-dimethyltricyclo[4.2.1.1(2,5)]decane-9,10-diol	0	0	0	0
2-pentadecanone, 6,10,14-trimethyl	1	1	1	1
Phytol	1	1	1	1
Isophytol	1	1	1	1
Z-(13,14-epoxy)tetradec-11-en-1-ol acetate	0	0	1	0
E,Z-1,3,12-nonadecatriene	0	0	1	0
7-methyl-Z-tetradecen-1-ol acetate	1	0	1	0
Ethyl iso-allocholate	1	3	0	1
Lupenone	1	1	0	1
4,22-cholestadien-3-one	2	4	0	1

An evaluation of the predicted toxicity of identified compounds in both the aqueous and methanolic/methylene chloride extracts was conducted. All compounds, except N-methyl-N-[4-[2-acetoxymethyl-1-pyrrolidyl]-2-butynyl]-acetamide, exhibited relatively high LD<sub>50</sub> values, indicating low acute toxicity. N-methyl-N-[4-[2-acetoxymethyl-1-pyrrolidyl]-2-butynyl]-acetamide displayed a predicted LD<sub>50</sub> of 41 mg/kg, placing it within Toxicity Class 2 (moderately toxic). *In silico* analysis also predicted potential carcinogenicity for 7-methyl-Z-tetradecen-1-ol acetate (prediction probability: 0.50) within the aqueous extract with LD<sub>50</sub> of 3460 mg/kg. Four compounds in the aqueous extract (ethyl iso-allocholate [0.57], trilinolein [0.57], olean-12-en-3-one [0.64], and  $\alpha$ -amyrin [0.98]) and three within the methanolic/methylene chloride extract (ethyl iso-allocholate [0.57], 4,22-cholestadien-3-one [0.99], and 3-acetoxy-7,8-epoxylanostan-11-ol [0.99]) showed predicted tendencies to induce immunotoxicity (prediction probability  $\geq 0.50$ ) (Tables XIII and XIV). While the majority of identified compounds pose minimal acute toxicity concerns, the predicted carcinogenicity and immunotoxicity of certain compounds warrant further investigation. In particular, 7-methyl-Z-tetradecen-1-ol acetate and the compounds identified with potential immunotoxicity should be subjected to more in-depth analysis to confirm or refute the *in silico* predictions.

**Table XIII.** Toxicological profile of phytochemicals from AES.

Phytochemicals	LD <sub>50</sub> (mg/kg) / Tox Class	Prediction accuracy (%)	Immunotoxicity	Carcinogenicity	Mutagenicity	Cytotoxicity
9-oxabicyclo[3.3.1]nonane-2,6-diol	3100 / 5	69.26	Inactive	Inactive	Inactive	Inactive
2,7-dioxaisotwistane	7800 / 6	69.26	Inactive	Inactive	Inactive	Inactive
5-hydroxy-9-oxabicyclo[3.3.1] nonan-2-one	20000 / 6	68.07	Inactive	Inactive	Inactive	Inactive
11-isopropylidenetricyclo[4.3.1.1(2,5)]undec-3-en-10-one	5000 / 5	69.26	Inactive	Inactive	Inactive	Inactive
4-(1,5-dihydroxy-2,6,6-trimethylcyclohex-2-enyl)but-3-en-2-one	1000 / 4	68.07	Inactive	Inactive	Inactive	Inactive
7-methyl-Z-tetradecen-1-ol acetate	3460 / 5	100	Inactive	Active (0.50)	Inactive	Inactive
ethyl iso-allocholate	5000 / 5	72.9	Active (0.57)	Inactive	Inactive	Inactive
Trilinolein	3700 / 6	70.97	Active (0.57)	Inactive	Inactive	Inactive
Olean-12-en-3-one	5000 / 5	72.9	Active (0.64)	Inactive	Inactive	Inactive
$\alpha$ -amyrin	7000 / 6	100	Active (0.98)	Inactive	Inactive	Inactive



**Table XIV.** Toxicological profile of phytochemicals from MES.

Phytochemicals	LD <sub>50</sub> (mg/kg) / Tox Class	Prediction accuracy (%)	Immunotoxicity	Carcinogenicity	Mutagenicity	Cytotoxicity
9-oxabicyclo[3.3.1]nonane-2,6-diol	3100 / 5	69.26	Inactive	Inactive	Inactive	Inactive
2,5-methano-2H-furo[3,2-b]pyran, hexahydro (2,7-dioxaisotwistane)	7800 / 6	69.26	Inactive	Inactive	Inactive	Inactive
6,6-dimethyl-10-methylene-1-oxa-spiro[4.5]decane	5000 / 5	69.26	Inactive	Inactive	Inactive	Inactive
N-methyl-N-[4-[2-acetoxymethyl-1-pyrrolidyl]-2-butynyl]-acetamide	41 / 2	68.07	Inactive	Inactive	Inactive	Inactive
9,10-dimethyltricyclo[4.2.1.1(2,5)]decane-9,10-diol	2000 / 4	70.97	Inactive	Inactive	Inactive	Inactive
2-pentadecanone, 6,10,14-trimethyl	5000 / 5	100.00	Inactive	Inactive	Inactive	Inactive
Phytol	5000 / 5	100.00	Inactive	Inactive	Inactive	Inactive
Isophytol	340 / 4	100.00	Inactive	Inactive	Inactive	Inactive
Z-(13,14-epoxy)tetradec-11-en-1-ol acetate	3460 / 5	70.97	Inactive	Active (0.63)	Active (0.58)	Inactive
E,Z-1,3,12-nonadecatriene	5000 / 5	70.97	Inactive	Inactive	Inactive	Inactive
7-methyl-Z-tetradecen-1-ol acetate	3460 / 5	100.00	Inactive	Active (0.50)	Inactive	Inactive
Ethyl iso-allocholate	5000 / 5	72.90	Active (0.57)	Inactive	Inactive	Inactive
Lupenone	2300 / 5	70.97	Inactive	Inactive	Inactive	Inactive
4,22-cholestadien-3-one	5000 / 5	72.90	Active (0.99)	Inactive	Inactive	Inactive

**Table XV** present the results of the *in silico* binding affinity (docking scores) of *E. speciosa* compounds against the profiled targets. The tested compounds generally displayed favorable binding affinities, with scores exceeding that of the standard control (-5.1 kcal/mol). Notably, 11-isopropylidenetricyclo[4.3.1.1(2,5)]undec-3-en-10-one exhibited the strongest binding affinity (-7.9 kcal/mol), while 2,7-dioxaisotwistane displayed the weakest affinity (-5.8 kcal/mol) within this set of compounds. However, it is important to note that acarbose, a well-established antidiabetic drug, demonstrated a slightly higher binding affinity (-7.7 kcal/mol) compared to the most potent *E. speciosa* compound. Interestingly, three compounds, 9,10-dimethyltricyclo[4.2.1.1(2,5)]decane-9,10-diol, 11-isopropylidenetricyclo[4.3.1.1(2,5)]undec-3-en-10-one, and 6,6-dimethyl-10-methylene-1-oxa-spiro[4.5]decane, shared the highest binding affinity among the tested compounds within a different target profile, with identical scores of -6.2 kcal/mol.

**Table XV.**  $\Delta G$  of top *E. speciosa* compounds with SGLT2 and  $\alpha$ -amylase.

Compounds	$\Delta G$ (kcal/mol)	
	SGLT2	$\alpha$ -amylase
2,7-dioxaisotwistane	-5.8	-4.6
9,10-dimethyltricyclo[4.2.1.1(2,5)]decane-9,10-diol	-6.6	-6.2
9-oxabicyclo[3.3.1]nonane-2,6-diol	-6.2	-5.4
11-isopropylidenetricyclo [4.3.1.1(2,5)]undec-3-en-10-one	-7.9	-7.1
4-(1,5-dihydroxy-2,6,6-trimethylcyclohex-2-enyl)but-3-en-2-one	-7.3	-6.2
5-hydroxy-9-oxabicyclo [3.3.1] nonan-2-one	-6.6	-5.4
6,6-dimethyl-10-methylene-1-oxa-spiro[4.5]decane	-6.5	-6.2
E,Z-1,3,12-nonadecatriene	-6.9	-5.2
N-methyl-N-[4-[2-acetoxymethyl-1-pyrrolidyl]-2-butynyl]-acetamide	-7.5	-6.0
Z-(13,14-epoxy)tetradec-11-en-1-ol acetate	-6.6	-5.6
Metformin	-5.1	-
Acarbose	-	-7.7

Docking simulations were validated to ensure the selected compounds bind to the SGLT2 protein at the same site as the co-crystallized (native) ligand (**Figure 1**). The 2D interaction diagrams for the top three compounds with SGLT2 are presented in **Figure 2**. 11-isopropylidenetricyclo[4.3.1.1(2,5)]undec-3-en-10-one formed nine interactions with SGLT2, primarily through van der Waals and alkyl bonds. Interacting amino acid residues included SER508, ALA446, ALA447, LEU452, PHE504, GLN448, GLN451, TYR455, and GLY507. 4-(1,5-dihydroxy-2,6,6-trimethylcyclohex-2-enyl)but-3-en-2-one exhibited 13 interactions with SGLT2, including two hydrogen bonds with PHE152 and SER156. Other interacting residues included ILE456, VAL443, VAL444, VAL459, TYR455, PHE504, GLN451, ALA447, LEU452, TRP440, and THR153. N-methyl-N-[4-[2-acetoxymethyl-1-pyrrolidyl]-2-butynyl]-acetamide displayed the most extensive network of interactions with SGLT2, forming 18 bonds, including three hydrogen bonds with TRP291, GLN457, and THR87. Additional interacting residues included SER287, ALA102, LYS321, ASN75, PHE98, PHE453, GLU99, VAL95, VAL157, VAL286, GLY79, GLY83, HIS80, LEU84, and TYR290.

Docking simulations were performed to investigate the potential interaction between  $\alpha$ -amylase and bioactive compounds identified in *E. speciosa*. The results for 4-(1,5-dihydroxy-2,6,6-trimethylcyclohex-2-enyl)but-3-en-2-one (compound name) are depicted in **Figure 3**. This compound exhibited thirteen interactions with  $\alpha$ -amylase, including two hydrogen bonds with ASP197 and THR163. Additional interacting residues involved in van der Waals forces included GLU233, ALA198, HIS101, TYR62, LEU165, LEU162, TRP59, TRP58, ASP300, HIS299, and ARG195. For comparison, the docking profile of acarbose, a known  $\alpha$ -amylase inhibitor, is presented in **Figure 4**. Acarbose displayed a higher number and wider variety of interactions with  $\alpha$ -amylase, including van der Waals forces, hydrogen bonds, and unfavorable donor-donor interactions. Molecular docking simulations were performed to assess the potential antidiabetic activity of *E. speciosa* compounds by evaluating their binding affinity to key diabetes-related targets: SGLT2 and  $\alpha$ -amylase<sup>32,33</sup>. Lower binding energy signifies stronger ligand-target interactions. All *E. speciosa* compounds displayed higher binding affinities for SGLT2 compared to metformin, a common antidiabetic drug. This suggests their potential as potent SGLT2 inhibitors, potentially reducing glucose reabsorption and mitigating diabetic kidney complications<sup>34,35</sup>. While the compounds exhibited lower binding affinities for  $\alpha$ -amylase compared to acarbose, another antidiabetic drug, a significant interaction was observed. This suggests their potential to inhibit  $\alpha$ -amylase activity and regulate postprandial glucose levels, making them promising candidates for diabetes management.

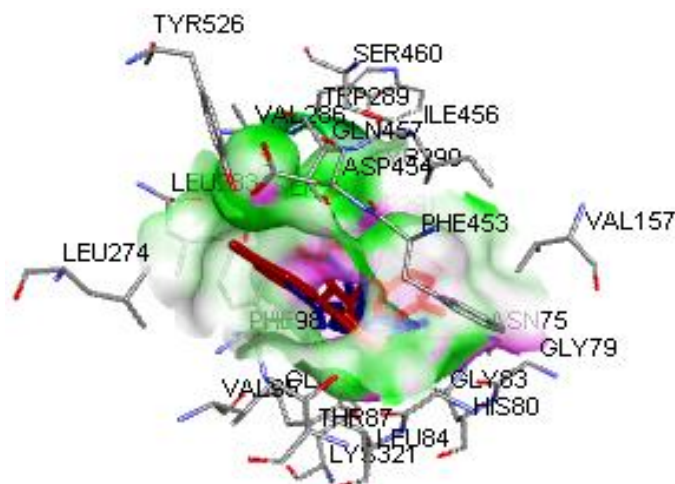


**Figure 1.** 3D structure of the super-imposition of N-methyl-N-[4-[2-acetoxymethyl-1-pyrrolidyl]-2-butynyl]-acetamide (red) and the native ligand (blue) in the binding pockets of SGLT2.

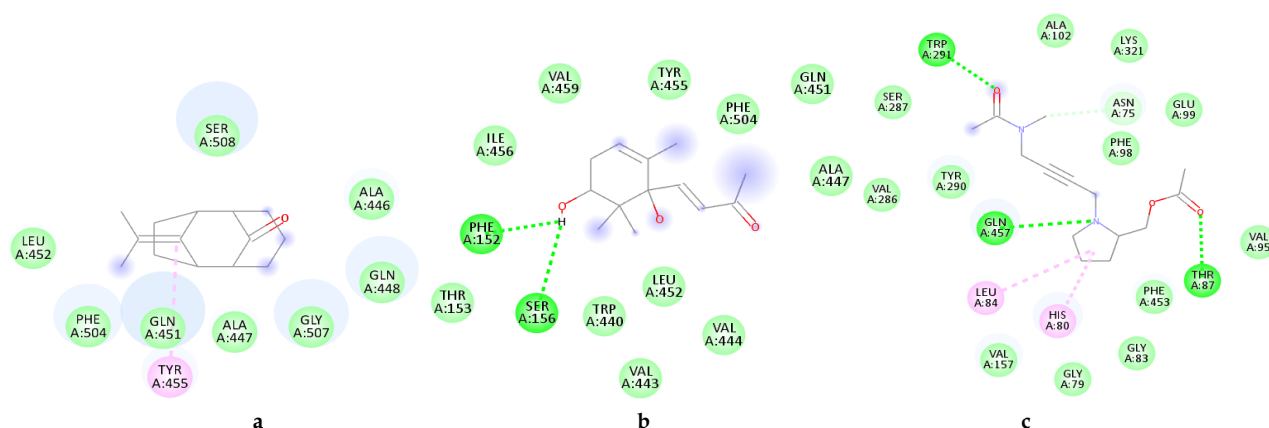


**Figure 2.** 2D binding interaction of 11-isopropylidene-tricyclo[4.3.1.1(2,5)]undec-3-en-10-one (a), 4-(1,5-dihydroxy-2,6,6-trimethylcyclohex-2-enyl)but-3-en-2-one (b), and N-methyl-N-[4-[2-acetoxymethyl-1-pyrrolidyl]-2-butynyl]-acetamide (c) with SGLT2. Van der Waals (light green), hydrogen (bright green), and Pi-alkyl (pink) interactions.

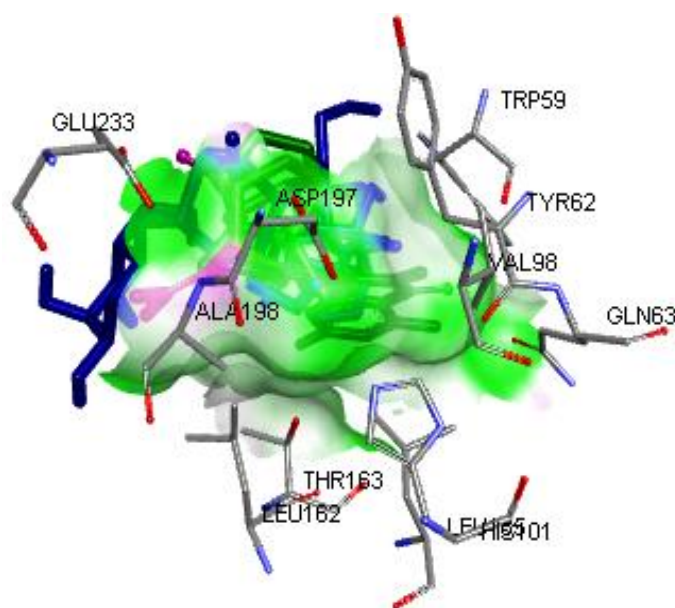


**Figure 3.** 3D structure of the super-imposition of 9,10-dimethyltricyclo[4.2.1.1(2,5)]decane-9,10-diol (red), 11-isopropylidene-tricyclo[4.3.1.1(2,5)]undec-3-en-10-one (purple), 6,6-dimethyl-10-methylene-1-oxa-spiro[4.5]decane (orange) and the native ligand (blue) in the binding pockets of  $\alpha$ -amylase.

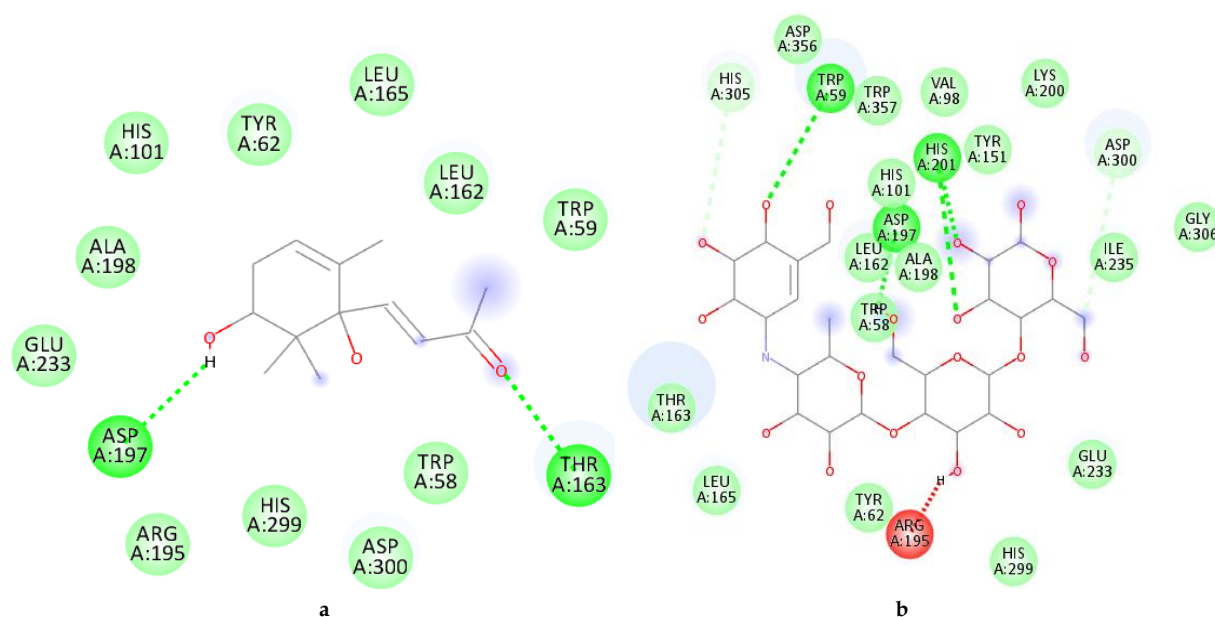


**Figure 4.** 2D binding interaction of 4-(1,5-dihydroxy-2,6,6-trimethylcyclohex-2-enyl)but-3-en-2-one (a) and acarbose (b) with  $\alpha$ -amylase. Van der Waals (light green), hydrogen (bright green), and unfavorable donor-donor (red) interactions.

Plant-based drug discovery is gaining significant interest due to the potential for lower toxicity and fewer side effects compared to synthetic medications<sup>36,37</sup>. However, the success of a compound as a therapeutic candidate is highly dependent on its physicochemical properties<sup>35</sup>. Here, we investigated the drug-likeness and antidiabetic potential of *E. speciosa* phytochemicals. This study identified *E. speciosa* phytochemicals with promising drug-like properties, low predicted toxicity, and potential for antidiabetic activity through SGLT2 and  $\alpha$ -amylase inhibition. Further *in vitro* and *in vivo* studies are warranted to validate these findings and explore their therapeutic potential for diabetes management.

## CONCLUSION

*In silico* assessment of *E. speciosa* compounds revealed promising drug-like properties and broad applicability in pharmaceutical development. The identified compounds exhibited a range of hydrophobicities, suggesting their potential

for various administration routes beyond oral delivery. This is further supported by the favorable bioavailability scores, placing them within the acceptable range for druggable candidates. Additionally, the *in silico* inhibition profiles against diabetic targets suggest a potential role for these compounds in diabetes management. However, further investigations are warranted to validate these findings. *In vitro* and *in vivo* studies are recommended to confirm the antidiabetic activity and establish the binding stability of the compounds with the identified diabetic targets.

## ACKNOWLEDGMENT

The authors gratefully acknowledge Siwe *et al.* for their significant contributions to this research.

## AUTHORS' CONTRIBUTION

**Conceptualization:** Sulyman Olalekan Ibrahim, Halimat Yusuf Lukman, Israel Ehizuelen Ebhohimen, Halimah Funmilayo Babamale, Abdulmumeen Amao Hamid, Marili Funmilayo Zubair, Olubunmi Atolani

**Data curation:** Sulyman Olalekan Ibrahim, Halimat Yusuf Lukman, Israel Ehizuelen Ebhohimen, Halimah Funmilayo Babamale, Fatimah Ronke Abdulkadir, Abdulmumeen Amao Hamid, Marili Funmilayo Zubair, Olubunmi Atolani

**Formal analysis:** Sulyman Olalekan Ibrahim, Halimat Yusuf Lukman, Israel Ehizuelen Ebhohimen, Halimah Funmilayo Babamale, Fatimah Ronke Abdulkadir, Abdulmumeen Amao Hamid, Marili Funmilayo Zubair, Olubunmi Atolani

**Funding acquisition:** -

**Investigation:** Sulyman Olalekan Ibrahim, Halimat Yusuf Lukman, Israel Ehizuelen Ebhohimen, Halimah Funmilayo Babamale, Fatimah Ronke Abdulkadir, Abdulmumeen Amao Hamid, Marili Funmilayo Zubair, Olubunmi Atolani

**Methodology:** Sulyman Olalekan Ibrahim, Halimat Yusuf Lukman, Israel Ehizuelen Ebhohimen, Halimah Funmilayo Babamale, Fatimah Ronke Abdulkadir, Abdulmumeen Amao Hamid, Marili Funmilayo Zubair, Olubunmi Atolani

**Project administration:** Sulyman Olalekan Ibrahim

**Resources:** Sulyman Olalekan Ibrahim, Olubunmi Atolani

**Software:** Sulyman Olalekan Ibrahim, Halimat Yusuf Lukman, Israel Ehizuelen Ebhohimen, Halimah Funmilayo Babamale, Abdulmumeen Amao Hamid, Marili Funmilayo Zubair, Olubunmi Atolani

**Supervision:** Sulyman Olalekan Ibrahim, Olubunmi Atolani

**Validation:** Sulyman Olalekan Ibrahim, Halimat Yusuf Lukman, Israel Ehizuelen Ebhohimen, Halimah Funmilayo Babamale, Abdulmumeen Amao Hamid, Marili Funmilayo Zubair, Olubunmi Atolani

**Visualization:** Sulyman Olalekan Ibrahim, Olubunmi Atolani

**Writing - original draft:** Sulyman Olalekan Ibrahim, Halimat Yusuf Lukman, Israel Ehizuelen Ebhohimen, Halimah Funmilayo Babamale, Fatimah Ronke Abdulkadir, Abdulmumeen Amao Hamid, Marili Funmilayo Zubair, Olubunmi Atolani

**Writing - review & editing:** Sulyman Olalekan Ibrahim, Halimat Yusuf Lukman, Israel Ehizuelen Ebhohimen, Halimah Funmilayo Babamale, Abdulmumeen Amao Hamid, Marili Funmilayo Zubair, Olubunmi Atolani

## DATA AVAILABILITY

None.

## CONFLICT OF INTEREST

The authors declare no conflicts of interest.

## REFERENCES

1. Andrade C, Gomes NG, Duangsrissai S, Andrade PB, Pereira DM, Valentao P. Medicinal plants utilized in Thai Traditional Medicine for diabetes treatment: ethnobotanical surveys, scientific evidence and phytochemicals. *J Ethnopharmacol.* 2020;263:113177. DOI: [10.1016/j.jep.2020.113177](https://doi.org/10.1016/j.jep.2020.113177); PMID: [32768637](https://pubmed.ncbi.nlm.nih.gov/32768637/)
2. Hussain A, Bhowmik B, do Vale Moreira NC. COVID-19 and diabetes: Knowledge in progress. *Diabetes Res Clin Pract.* 2020;162:108142. DOI: [10.1016/j.diabres.2020.108142](https://doi.org/10.1016/j.diabres.2020.108142); PMCID: [PMC7144611](https://pubmed.ncbi.nlm.nih.gov/PMC7144611/); PMID: [32278764](https://pubmed.ncbi.nlm.nih.gov/32278764/)
3. Rachdaoui N. Insulin: the friend and the foe in the development of type 2 diabetes mellitus. *Int J Mol Sci.* 2020;21(5):1770. DOI: [10.3390/ijms21051770](https://doi.org/10.3390/ijms21051770); PMCID: [PMC7084909](https://pubmed.ncbi.nlm.nih.gov/PMC7084909/); PMID: [32150819](https://pubmed.ncbi.nlm.nih.gov/32150819/)
4. Hameed I, Masoodi SR, Mir SA, Nabi M, Ghazanfar K, Ganai BA. Type 2 diabetes mellitus: from a metabolic disorder to an inflammatory condition. *World J Diabetes.* 2015;6(4):598-612. DOI: [10.4239/wjd.v6.i4.598](https://doi.org/10.4239/wjd.v6.i4.598); PMCID: [PMC4434080](https://pubmed.ncbi.nlm.nih.gov/PMC4434080/); PMID: [25987957](https://pubmed.ncbi.nlm.nih.gov/25987957/)
5. Galicia-Garcia U, Benito-Vicente A, Jebari S, Larrea-Sebal A, Siddiqi H, Uribe KB, et al. Pathophysiology of Type 2 Diabetes Mellitus. *Int J Mol Sci.* 2020;21(17):6275. DOI: [10.3390/ijms21176275](https://doi.org/10.3390/ijms21176275); PMCID: [PMC7503727](https://pubmed.ncbi.nlm.nih.gov/PMC7503727/); PMID: [32872570](https://pubmed.ncbi.nlm.nih.gov/32872570/)
6. Sacks KN, Friger M, Shoham-Vardi I, Abokaf H, Spiegel E, Sergienko R, et al. Prenatal exposure to gestational diabetes mellitus as an independent risk factor for long-term neuropsychiatric morbidity of the offspring. *Am J Obstet Gynecol.* 2016;215(3):380.e1-7. DOI: [10.1016/j.ajog.2016.03.030](https://doi.org/10.1016/j.ajog.2016.03.030); PMID: [27018463](https://pubmed.ncbi.nlm.nih.gov/27018463/)
7. Astutik S, Pretzsch J, Kimengsi JN. Asian medicinal plants' production and utilization potentials: A review. *Sustainability.* 2019;11(19):5483. DOI: [10.3390/su11195483](https://doi.org/10.3390/su11195483)
8. Pundarikakshudu K, Shah PA, Patel MG. Chapter 1 - A comprehensive review of Indian medicinal plants effective in diabetes management: Current status and future prospects. In: Naeem M, Aftab T, editors. *Antidiabetic Medicinal Plants: Applications and Opportunities.* Cambridge; Academic Press: 2024. p. 3-73. DOI: [10.1016/B978-0-323-95719-9.00013-6](https://doi.org/10.1016/B978-0-323-95719-9.00013-6)
9. Nchegang B, Mezui C, Longo F, Nkwengoua Z, Amang A, Tan P. Effects of the aqueous extract of *Eremomastax speciosa* (Acanthaceae) on sexual behavior in normal male rats. *Biomed Res Int.* 2016;2016:9706429. DOI: [10.1155/2016/9706429](https://doi.org/10.1155/2016/9706429); PMCID: [PMC4971301](https://pubmed.ncbi.nlm.nih.gov/PMC4971301/); PMID: [27525283](https://pubmed.ncbi.nlm.nih.gov/27525283/)
10. Effiong GS, Ebe NU, Akpanyung EO, Emeka RA, Nwuzor EO. Effects of Ethanol Leaf Extract of *Eremomastax speciosa* (African Blood Tonic) on Female Reproductive Hormones of Albino Wistar Rats. *Int J Biochem Bioinform Biotechnol Stud.* 2020;5(1):1-12.
11. Onoja SO, Eke C, Ejiofor E, Madubuike KG, Ezeja MI, Omeh YN, et al. antioxidant, anti-inflammatory and anti-nociceptive properties of hydro-methanol extract of *Eremomastax speciosa* (Hochst.) Cufod leaf. *Afr J Tradit Complement Altern Med.* 2017;14(6):56-63. DOI: [10.21010/ajtcam.v14i6.6](https://doi.org/10.21010/ajtcam.v14i6.6)
12. Barlow D, Buriani A, Ehrman T, Bosisio E, Eberini I, Hylands P. In-silico studies in Chinese herbal medicines' research: evaluation of in-silico methodologies and phytochemical data sources, and a review of research to date. *J Ethnopharmacol.* 2012;140(3):526-34. DOI: [10.1016/j.jep.2012.01.041](https://doi.org/10.1016/j.jep.2012.01.041); PMCID: [PMC7126886](https://pubmed.ncbi.nlm.nih.gov/PMC7126886/); PMID: [22326356](https://pubmed.ncbi.nlm.nih.gov/22326356/)
13. Ibrahim SO, Lukman HY, Zubair MF, Amusan OT, Abdulkadri FR, Lawal B, et al. An Insight into the Physicochemical, Drug-likeness, Pharmacokinetics and Toxicity Profile of *Kigelia africana* (Lam) Bioactive Compounds. *Al-Bahir J Eng Pure Sci.* 2024;4(1):4. DOI: [10.55810/2313-0083.1050](https://doi.org/10.55810/2313-0083.1050)
14. Rehman A, Bukhari SA, Akhter N, Hussain MAI, Chaudhary Z. In Silico identification of novel phytochemicals that target SFRP4: An early biomarker of diabetes. *PLoS One.* 2023;18(11):e0292155. DOI: [10.1371/journal.pone.0292155](https://doi.org/10.1371/journal.pone.0292155); PMCID: [PMC10635506](https://pubmed.ncbi.nlm.nih.gov/PMC10635506/); PMID: [37943820](https://pubmed.ncbi.nlm.nih.gov/37943820/)

15. Jamtsho T, Yeshi K, Perry MJ, Loukas A, Wangchuk P. Approaches, Strategies and Procedures for Identifying Anti-Inflammatory Drug Lead Molecules from Natural Products. *Pharmaceutics*. 2024;17(3):283. DOI: [10.3390/ph17030283](https://doi.org/10.3390/ph17030283); PMCID: [PMC10974486](https://pubmed.ncbi.nlm.nih.gov/38543070/); PMID: [38543070](https://pubmed.ncbi.nlm.nih.gov/38543070/)
16. Siwe GT, Ernestine NZ, Amang A, Mezui C, Choudhary I, Tan P. Comparative GC-MS analysis of two crude extracts from *Eremomastax speciosa* (Acanthaceae) leaves. *J Med Plant Stud*. 2019;7(2):25-9.
17. Daina A, Michielin O, Zoete V. SwissADME: a free web tool to evaluate pharmacokinetics, drug-likeness and medicinal chemistry friendliness of small molecules. *Sci Rep*. 2017;7(1):42717. DOI: [10.1038/srep42717](https://doi.org/10.1038/srep42717); PMCID: [PMC5335600](https://pubmed.ncbi.nlm.nih.gov/28256516/); PMID: [28256516](https://pubmed.ncbi.nlm.nih.gov/28256516/)
18. Banerjee P, Eckert AO, Schrey AK, Preissner R. ProTox-II: a webserver for the prediction of toxicity of chemicals. *Nucleic Acids Res*. 2018;46(W1):W257-63. DOI: [10.1093/nar/gky318](https://doi.org/10.1093/nar/gky318); PMCID: [PMC6031011](https://pubmed.ncbi.nlm.nih.gov/29718510/); PMID: [29718510](https://pubmed.ncbi.nlm.nih.gov/29718510/)
19. Kalra S, Jacob J, Baruah MP. Metformin + Sodium-glucose Co-transporter-2 Inhibitor: Salutogenic Lifestyle Mimetics in a Tablet? *Indian J Endocrinol Metab*. 2018;22(1):164-6. DOI: [10.4103/ijem.ijem\\_266\\_17](https://doi.org/10.4103/ijem.ijem_266_17); PMCID: [PMC5838898](https://pubmed.ncbi.nlm.nih.gov/29535955/); PMID: [29535955](https://pubmed.ncbi.nlm.nih.gov/29535955/)
20. Oboh G, Ogunsuyi OB, Ogunbadejo MD, Adefegha SA. Influence of gallic acid on  $\alpha$ -amylase and  $\alpha$ -glucosidase inhibitory properties of acarbose. *J Food Drug Anal*. 2016;24(3):627-34. DOI: [10.1016/j.jfda.2016.03.003](https://doi.org/10.1016/j.jfda.2016.03.003); PMCID: [PMC9336674](https://pubmed.ncbi.nlm.nih.gov/28911570/); PMID: [28911570](https://pubmed.ncbi.nlm.nih.gov/28911570/)
21. Trott O, Olson AJ. AutoDock Vina: improving the speed and accuracy of docking with a new scoring function, efficient optimization, and multithreading. *J Comput Chem*. 2010;31(2):455-61. DOI: [10.1002/jcc.21334](https://doi.org/10.1002/jcc.21334); PMCID: [PMC3041641](https://pubmed.ncbi.nlm.nih.gov/19499576/); PMID: [19499576](https://pubmed.ncbi.nlm.nih.gov/19499576/)
22. Antoni C, Vera L, Devel L, Catalani MP, Czarny B, Cassar-Lajeunesse E, et al. Crystallization of bi-functional ligand protein complexes. *J Struct Biol*. 2013;182(3):246-54. DOI: [10.1016/j.jsb.2013.03.015](https://doi.org/10.1016/j.jsb.2013.03.015); PMID: [23567804](https://pubmed.ncbi.nlm.nih.gov/23567804/)
23. Aribisala JO, Sabiu S. Cheminformatics identification of phenolics as modulators of penicillin-binding protein 2a of *Staphylococcus aureus*: A structure-activity-relationship-based study. *Pharmaceutics*. 2022;14(9):1818. DOI: [10.3390/pharmaceutics14091818](https://doi.org/10.3390/pharmaceutics14091818); PMCID: [PMC9503099](https://pubmed.ncbi.nlm.nih.gov/36145565/); PMID: [36145565](https://pubmed.ncbi.nlm.nih.gov/36145565/)
24. Manaia EB, Abuçafy MP, Chiari-Andréo BG, Silva BL, Junior JAO, Chiavacci LA. Physicochemical characterization of drug nanocarriers. *Int J Nanomedicine*. 2017;12:4991-5011. DOI: [10.2147/ijn.s133832](https://doi.org/10.2147/ijn.s133832); PMCID: [PMC5516877](https://pubmed.ncbi.nlm.nih.gov/28761340/); PMID: [28761340](https://pubmed.ncbi.nlm.nih.gov/28761340/)
25. Saravanakumar A, Sadighi A, Ryu R, Akhlaghi F. Physicochemical properties, biotransformation, and transport pathways of established and newly approved medications: a systematic review of the top 200 most prescribed drugs vs. the FDA-approved drugs between 2005 and 2016. *Clin Pharmacokinet*. 2019;58(10):1281-94. DOI: [10.1007/s40262-019-00750-8](https://doi.org/10.1007/s40262-019-00750-8); PMCID: [PMC6773482](https://pubmed.ncbi.nlm.nih.gov/30972694/); PMID: [30972694](https://pubmed.ncbi.nlm.nih.gov/30972694/)
26. Kadri A, Aouadi K. In vitro antimicrobial and  $\alpha$ -glucosidase inhibitory potential of enantiopure cycloalkylglycine derivatives: Insights into their in silico pharmacokinetic, druglikeness, and medicinal chemistry properties. *J Appl Pharm Sci*. 2020;10(6):107-15. DOI: [10.7324/JAPS.2020.10614](https://doi.org/10.7324/JAPS.2020.10614)
27. Lipinski CA. Lead-and drug-like compounds: the rule-of-five revolution. *Drug Discov Today Technol*. 2004;1(4):337-41. DOI: [10.1016/j.ddtec.2004.11.007](https://doi.org/10.1016/j.ddtec.2004.11.007); PMID: [24981612](https://pubmed.ncbi.nlm.nih.gov/24981612/)
28. Riaz M, Zia-Ul-Haq M, Saad B. Anthocyanins and human health: biomolecular and therapeutic aspects. Cham: Springer; 2016. DOI: [10.1007/978-3-319-26456-1](https://doi.org/10.1007/978-3-319-26456-1)
29. Ahmed AH, Alkali YI. In silico pharmacokinetics and molecular docking studies of lead compounds derived from *Diospyros mespiliformis*. *PharmaTutor*. 2019;7(3):31-7. DOI: [10.29161/PT.v7.i3.2019.31](https://doi.org/10.29161/PT.v7.i3.2019.31)

30. Welcome MO. Blood brain barrier inflammation and potential therapeutic role of phytochemicals. *PharmaNutrition*. 2020;11:100177. DOI: [10.1016/j.phanu.2020.100177](https://doi.org/10.1016/j.phanu.2020.100177)
31. Pardridge WM. Drug transport across the blood–brain barrier. *J Cereb Blood Flow Metab*. 2012;32(11):1959-72. DOI: [10.1038/jcbfm.2012.126](https://doi.org/10.1038/jcbfm.2012.126); PMCID: [PMC3494002](https://pubmed.ncbi.nlm.nih.gov/PMC3494002/); PMID: [22929442](https://pubmed.ncbi.nlm.nih.gov/22929442/)
32. Pinzi L, Rastelli G. Molecular docking: shifting paradigms in drug discovery. *Int J Mol Sci*. 2019;20(18):4331. DOI: [10.3390/ijms20184331](https://doi.org/10.3390/ijms20184331); PMCID: [PMC6769923](https://pubmed.ncbi.nlm.nih.gov/PMC6769923/); PMID: [31487867](https://pubmed.ncbi.nlm.nih.gov/31487867/)
33. Jiao X, Jin X, Ma Y, Yang Y, Li J, Liang L, et al. A comprehensive application: Molecular docking and network pharmacology for the prediction of bioactive constituents and elucidation of mechanisms of action in component-based Chinese medicine. *Comput Biol Chem*. 2021;90:107402. DOI: [10.1016/j.combiolchem.2020.107402](https://doi.org/10.1016/j.combiolchem.2020.107402); PMID: [33338839](https://pubmed.ncbi.nlm.nih.gov/33338839/)
34. Gong L, Feng D, Wang T, Ren Y, Liu Y, Wang J. Inhibitors of  $\alpha$ -amylase and  $\alpha$ -glucosidase: Potential linkage for whole cereal foods on prevention of hyperglycemia. *Food Sci Nutr*. 2020;8(12):6320-37. DOI: [10.1002/fsn3.1987](https://doi.org/10.1002/fsn3.1987); PMCID: [PMC7723208](https://pubmed.ncbi.nlm.nih.gov/PMC7723208/); PMID: [33312519](https://pubmed.ncbi.nlm.nih.gov/33312519/)
35. Swain SS, Hussain T. Combined Bioinformatics and Combinatorial Chemistry Tools to Locate Drug-Able Anti-TB Phytochemicals: A Cost-Effective Platform for Natural Product-Based Drug Discovery. *Chem Biodivers*. 2022;19(11):e202200267. DOI: [10.1002/cbdv.202200267](https://doi.org/10.1002/cbdv.202200267)
36. Nasim N, Sandeep IS, Mohanty S. Plant-derived natural products for drug discovery: current approaches and prospects. *Nucleus*. 2022;65(3):399-411. DOI: [10.1007/s13237-022-00405-3](https://doi.org/10.1007/s13237-022-00405-3); PMCID: [PMC9579558](https://pubmed.ncbi.nlm.nih.gov/PMC9579558/); PMID: [36276225](https://pubmed.ncbi.nlm.nih.gov/36276225/)
37. Vaou N, Stavropoulou E, Voidarou C, Tsigalou C, Bezirtzoglou E. Towards Advances in Medicinal Plant Antimicrobial Activity: A Review Study on Challenges and Future Perspectives. *Microorganisms*. 2021;9(10):2041. DOI: [10.3390/microorganisms9102041](https://doi.org/10.3390/microorganisms9102041); PMCID: [PMC8541629](https://pubmed.ncbi.nlm.nih.gov/PMC8541629/); PMID: [34683362](https://pubmed.ncbi.nlm.nih.gov/34683362/)